

Optimizing Ultra-High-Performance Fiber-Reinforced Concrete

Mixtures with twisted fibers exhibit record performance under tensile loading

by Kay Wille, Antoine E. Naaman, and Sherif El-Tawil

Ultra-high-performance concrete (UHPC) has attracted the attention of researchers and practitioners since its introduction in the mid-1990s, not only because of its high compressive strength (generally exceeding 150 MPa [22 ksi]) but also because of its excellent environmental resistance.¹ The proper addition of fibers to UHPC further improves tensile cracking resistance, post-cracking strength, ductility, and energy absorption capacity. The tensile strength of an ultra-high-performance fiber-reinforced concrete (UHP-FRC) using small-diameter, high-strength, short, smooth steel fibers has been reported to range from about 8 to 15 MPa (1.2 to 2.2 ksi).²⁻⁷ Strain values reported from direct tensile tests range from 0.1 to 0.3%, but little information exists on its tensile strain capacity after cracking.

The research reported in this article focused on optimizing a UHP-FRC mixture for tensile strength, tensile strain capacity, and energy absorption—the key parameters relative to the performance of structural members. This was achieved by optimizing the cementitious matrix for compressive strength, packing density, and flowability; using very-high-strength, fine-diameter steel fibers; and tailoring the mechanical bond between the fiber and the cement matrix. The mixtures were mixed using a commercial mixer,⁸ and they were evaluated by measuring spread, compressive strength, single fiber pullout resistance, and direct tensile strength (Fig. 1).

Compressive Strength

High particle packing density (low matrix porosity) is a key property of ultra-high compressive strength concrete. In this research, a UHPC with a compressive strength exceeding 200 MPa (30 ksi) was developed using commercially available materials and without the use of any heat treatment, pressure curing, or a special mixer.

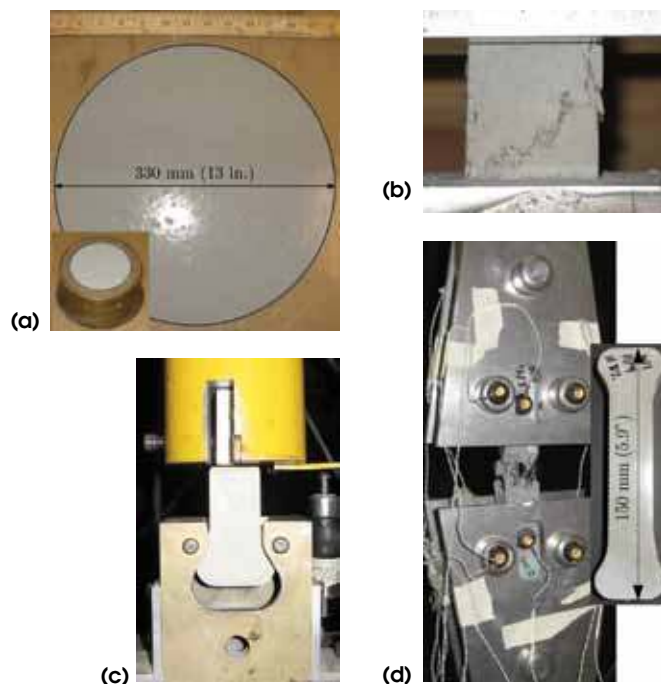


Fig. 1: Test methods used for developing UHP-FRC mixtures: (a) spread test; (b) compression test; (c) fiber pullout test; and (d) tensile test

The UHPC mixture design was based on optimizing the particle packing density of sand, silica fume, glass powder, and cement. The mixtures were evaluated by measuring the spread and the amount of entrapped air.^{8,9} Improving particle packing density was achieved mainly by changing the matrix composition and proportions, and by selecting ranges of particle sizes for sand, silica fume, glass powder, and cement. One mixture proportion selected as a baseline for the production of UHP-FRC is given in

Table 1. With the addition of high-strength steel fibers, 28-day compressive strengths of up to 291 MPa (42.3 ksi) were attained.

Tensile Strength, Ductility, and Formation of Multiple Cracks

The tensile strength σ_{pc} of UHP-FRC is defined by the engineering stress at maximum tensile load. Ductility is defined by the ability to deform plastically prior to tensile fracture. It can be evaluated by the strain ϵ_{pc} at σ_{pc} ,⁹ by the ductility index $I_d = E_{cc}\epsilon_{pc}/\sigma_{pc}$,¹⁰ which includes the elastic modulus E_{cc} , or by the dissipated energy per unit volume $g_{f,A}$ (explained in more detail in a following section and Fig. 2(b)).⁷

By definition, a strain-hardening UHP-FRC develops a σ_{pc} in excess of its first cracking strength σ_{cc} . A key factor leading to enhanced ductility and dissipation of energy is the formation of multiple cracks (Fig. 2). Although ductility generally decreases with increased tensile strength,¹¹ we attempted to find a UHP-FRC design that exhibited concurrent increases in both tensile strength and ductility.

Table 1:
Mixture proportions by weight

Type	UHPC	UHP-FRC	SIFCON
Cement	1.00	1.00	1.00
Silica fume	0.25	0.25	0.25
Glass powder	0.25	0.25	0.25
Water	0.180	0.18 to 0.20	0.207
High-range water-reducing admixture*	0.0114	0.0108	0.0108
Sand A†	1.05	0.92	0.83
Fiber	0.00	0.22 to 0.31	0.49
Fiber, vol. %	0	2.5 to 3.5	5.5
f'_c , MPa‡	232 to 246	251 to 291	270
f_t , MPa	8.2 to 9.0§	20 to 30	37

*Solid content

†Maximum grain size 0.2 mm

‡28-day tests using 50 mm cubes

§At first cracking, followed by immediate failure

1 MPa = 145 psi; 1 mm = 0.04 in.

FIXconcrete.org

Access over 1000 Videos Dedicated to the Repair, Protection, and Upgrade of Concrete Structures:

FixConcrete.org is a simple and easy-to-use tool comprising video presentations. The system currently has **more than 1000 technical presentations** from ACI and ICRI conventions.

FixConcrete.org Benefits:

- Retrieve knowledge anywhere, anytime on the Web by browsing or using a keyword search
- View technical information presented by industry leaders
- Learn about new technology and procedures
- Watch video presentations in real time with streaming video

FixConcrete.org Sponsored By:

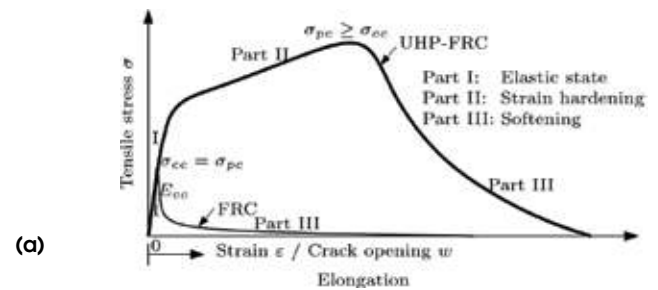


aci
American Concrete Institute®
Advancing concrete knowledge

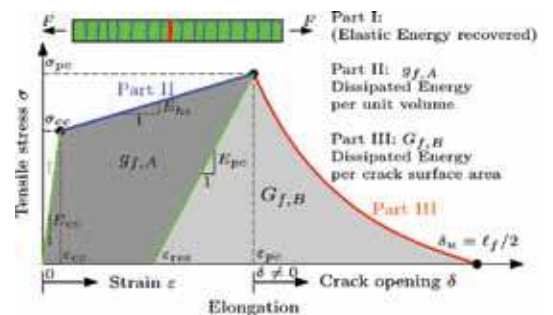


**INTERNATIONAL
CONCRETE REPAIR
INSTITUTE**

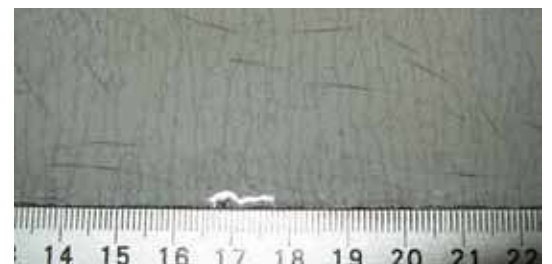
To register for this FREE service, go to www.fixconcrete.org



(a)



(b)



(c)

Fig. 2: Strain hardening tensile behavior of UHP-FRC: (a) strain-hardening versus strain-softening tensile response; (b) idealized tensile response and energy approach; and (c) multiple cracking of UHP-FRC with twisted fibers at 1.5 vol.%

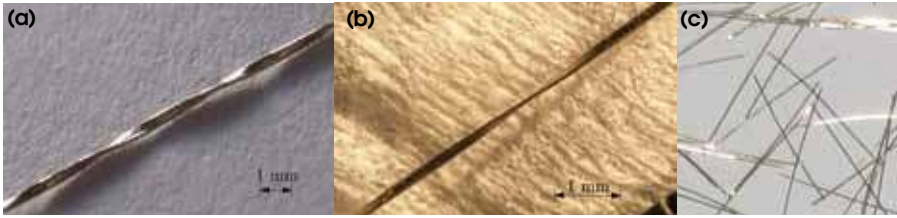


Fig. 3: Fibers used in the study: (a) twisted (T30) equivalent $d_f = 0.3$ mm (0.01 in.); (b) twisted (T12) equivalent $d_f = 0.12$ mm (0.005 in.); and (c) straight (S20) $d_f = 0.2$ mm (0.008 in.)

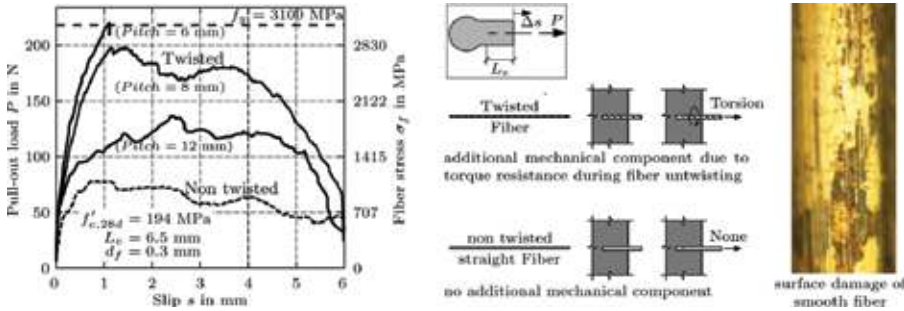


Fig. 4: Pullout characteristics of twisted and non-twisted fibers (1 N = 0.225 lb.; 1 mm = 0.04 in.)

Steel Fibers

We selected steel fibers for our UHP-FRC mixtures because steel's plastic behavior allows customization of fiber geometries and its high elastic modulus helps minimize crack widths in concrete. Three types of fibers were used in this study:

- Rectangular twisted steel fibers, produced from 0.3 mm (0.01 in.) diameter base wire (Fig. 3(a)) with a tensile strength of 3100 MPa (449 ksi). The mechanical bond of twisted fibers is activated during fiber pullout by torque resistance distributed along the fiber length. By varying the cross-sectional shape and the pitch of the fiber twist, we were able to modify the ratio of fiber surface to cross-sectional areas, the fiber torque resistance, and the angle of fiber-matrix interface, thereby adjusting the fiber-matrix mechanical bond;
- Micro-twisted steel fibers, produced from 0.12 mm (0.005 in.) diameter base wire (Fig. 3(b)) with a tensile strength of more than 3500 MPa (507 ksi). This fiber type was designed to improve the tensile cracking behavior of UHP-FRC with relatively low fiber volume content V_f . Production of this fiber type required overcoming a number of technical challenges associated with shaping, twisting, pulling, and cutting small diameter wire; and
- Commercially available smooth brass-coated 0.20 mm (0.008 in.) diameter steel fibers. The fibers were 13 mm (0.5 in.) long and had a tensile strength of 2600 MPa (377 ksi) (Fig. 3(c)). This type of fiber has been used in many UHP-FRC mixtures, and it is known to provide a good trade-off between tensile properties and workability of the fiber composite.

Single Fiber Pullout

Single fiber pullout tests were carried out using a procedure described in detail in Reference 12. Figure 4 illustrates the different pullout load-versus-slip performance of single twisted fibers embedded in UHPC in comparison to non-twisted fibers of the same material, embedment length, and fiber cross section. The twist ratio was tailored to achieve the highest tensile stress without inducing fiber failure. Optimized twisting leads to a tensile stress (and thus bond strength) increase of about two-and-a-half times without loss in the “ductile” nature of the pullout load-versus-slip behavior.

Inspection of the lower curve in Fig. 4 indicates that the smooth, 0.3 mm (0.01 in.) diameter fiber had an excellent load-versus-slip

behavior up to about the full embedded length. This has also been confirmed on smooth, 0.2 mm (0.008 in.) diameter microfibers.¹² Similar results on the same type of microfiber embedded in heat-treated UHPC were reported in References 13 and 14. Microscopic analysis of the pulled-out fibers showed that the brass coating layer at the fiber surface was damaged in many places (Fig. 4). Further analyses suggested that three effects may explain such behavior: a wedge effect of adhered and abraded particles at the interface; damage at the fiber surface; and deformation at the fiber ends caused by the shearing of the fibers during production, which provides mechanical anchorage.¹²

Direct Tensile Tests

Direct tensile tests were carried out on dog-bone-shaped, unnotched specimens. As outlined in Table 2, the specimens are categorized into two groups according to fiber factor χ_f , where $\chi_f = (\text{fiber length}/\text{fiber diameter}) \times V_f$.

The UHP-FRC mixtures of Group A have χ_f values of 2.0 or less (References 15 and 16) and are characterized by excellent workability with self-consolidating properties. The UHP-FRC mixtures of Group B have χ_f values greater than 2.0. These mixtures were more difficult to mix than Group A mixtures and more effort was required to place them in the molds. The highest value of χ_f (4.4) was achieved by filling the mold with fibers and infiltrating the fiber network with the cementitious matrix—a process known as SIFCON.^{17,18} All specimens, except UHP-FRC Sifcon-T30 5.5%, were cast in layers, which led to a preferable alignment of the fibers in the direction of the axis of the specimen (thus, the applied load).

Table 2:
Tensile parameters of UHP-FRC mixtures

	Type	$f'_c, 28, \text{MPa}$	l_f, mm	d_f, mm	$V_f, \%$	χ_f	σ_{pc}, MPa	$\epsilon_{pc}, \%$	l_d^a	$g_{f,A}, \text{kJ/m}^3$	$G, \text{kJ/m}^3$
Group A	Ceracem	191	20	0.30	2.5	1.7	9.7	0.25	15	20	25
	Ductal	200 [†]	13	0.20	2.0	1.3	12.0	0.07/0.3 [†]	3	—	—
	T12 1%	254	22	0.12	1.0	1.8	15.9	1.00	38	92	128
	T12 1.5%	255	15	0.12	1.5	1.9	18.9	0.83	26	94	129
	S 3%	254	13	0.20	3.0	2.0	20.0	0.59	18	88	115
Group B	CARDIFRC	185	6/13	0.16	4.5/1.5	2.9	13.5	0.06	3	—	—
	CEMTEC _{multiscale}	220 [‡]	Three fiber types	Three fiber types	11.0	—	20.0	0.20	6	—	—
	T12 2.3%	255	15	0.12	2.3	2.9	23.4	0.81	21	105	148
	T12 3%	254	22/24	0.12/0.3	1.0/2.0	3.4	31.1	0.72	14	106	168
	T12 6%	250	10/15/24	0.12/0.3/0.3	1.8/3.7/0.9	4.1	34.6	0.46	8	77	125
	Sifcon-T30 5.5%	270	24	0.30	5.5	4.4	37.2	1.08	17	169	304

Ceracem, Ductal, CARDIFRC, and CEMTEC data are from References 6, 4, 5, and 19, respectively; [†]Heat treatment with 90°C; [‡]Calculated from diagrams in References 4 and 20; [§] $E_c = 60 \text{ GPa}$ used in calculation; 1 MPa = 145 psi; 1 mm = 0.04 in.; 1°C = 34°F

The typical tensile behavior of the two groups of UHP-FRCs is presented in Fig. 5. For each mixture type, three to five specimens were tested. In Fig. 5(a), the tensile behavior of three different UHP-FRC types of Group A are compared to tensile test results of UHP-FRCs reported by other researchers identified in the footnote of Table 2. Higher tensile strength and an improvement in strain at maximum stress have been achieved while using a smaller volume fraction of fibers.

Commercially available straight steel fibers (S20, Fig. 3(a)) with a volume fraction of 3% resulted in a tensile strength of 20 MPa (2.9 ksi) associated with a strain value at peak stress $\epsilon_{pc} = 0.6\%$. This is three to ten times the strain value reported by others for their UHP-FRCs (Table 2). Similar tensile strength (19 MPa [3.2 ksi]) and improved ductility was obtained by using 15 mm (0.59 in.) long twisted fibers at a volume fraction of only 1.5%. Using 22 mm (0.87 in.) long twisted fibers and at a volume fraction of 1% (Type T12 1%) led to a post-cracking tensile strength of 15.9 MPa (2.3 ksi) and an impressive strain at a peak stress of 1%. The ductility index l_d was 38 for mixture Type T12 1%. This is about three to 12 times higher than that of other UHP-FRCs, and it exceeds the maximum value of 30 reported by Rossi.¹⁰ Assuming fiber failure is prevented, the results presented in Fig. 5(a) suggest that longer fibers improve the composite ductility.

Figure 5(b) describes the stress-strain response of four mixture types in Group B. Type T12 2.3% incorporates the same fine twisted steel fiber type as Type T12 1.5% in Group A. It develops a higher tensile strength of

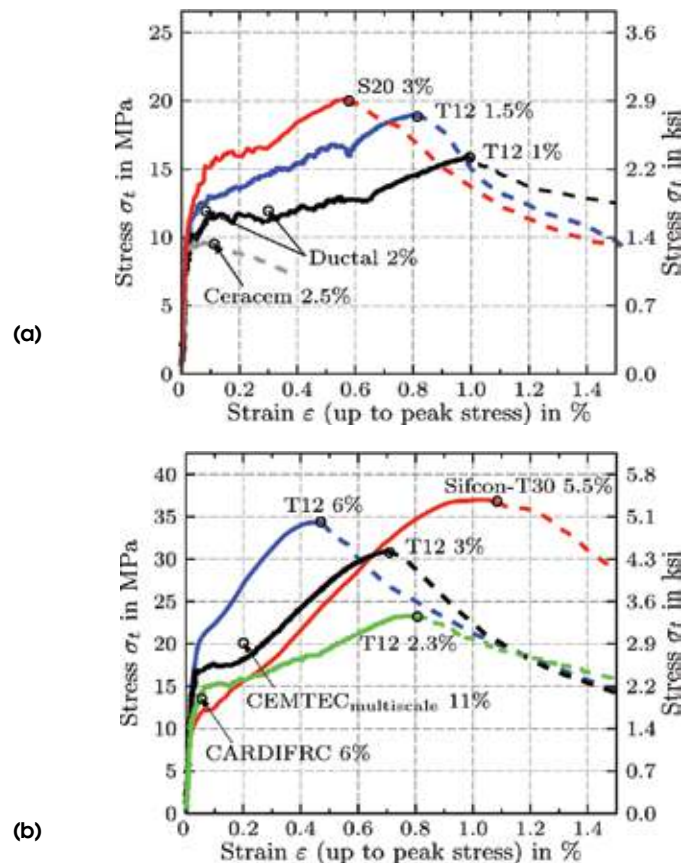


Fig. 5: Tensile behavior of UHP-FRCs developed in this research in comparison to results reported by other researchers: (a) UHP-FRCs of good workability (Group A); and (b) UHP-FRCs of difficult workability but very high tensile strength (Group B)

23.4 MPa (3.4 ksi) due to the increase in fiber volume fraction. The strain values are slightly over 0.8% for both mixture types.

To further optimize the tensile response of the composite, a blend of fibers of different lengths and diameters was used in series T12 3% and T12 6% (Table 2). A fiber blend allows mixtures to have higher volume fractions of fibers. Type T12 3% developed a tensile strength of 31.1 MPa (4.5 ksi) at a strain of 0.72%, whereas Type T12 6% developed a tensile strength of 34.6 MPa (5.0 ksi) at a strain of only 0.46%. These results indicate that higher total fiber content may lead only to a marginal increase in the tensile strength and even a decrease in ductility. Figure 5(b) also shows the performance of Type Sifcon-T30 5.5% by volume. The results ($\sigma_{pc} = 37.2$ MPa [5.4 ksi] and $\varepsilon_{pc} = 1.08\%$) are the best overall for both strength and strain capacity. Although SIFCON may not have the potential for widespread applications, the performance of this mixture type illustrates the upper limits of the tensile strength achievable in a discontinuous fiber-reinforced cementitious composite.

In Fig. 5(b), a point is shown for CEMTEC_{multiscale}[®], a UHP-FRC with a steel fiber content of 11%.²¹ It can be observed that results achieved ($\sigma_{pc} = 20$ MPa [2.9 ksi] and $\varepsilon_{pc} = 0.2\%$) are lower than values obtained for series T12 3%, which has about one-fourth the total fiber content.

Energy Absorption Capacity

In a previous study, distinguishing between the energy dissipated up to the end of strain-hardening behavior (that is, the peak load) and the energy associated with the softening behavior after localization (Fig. 2(b)) was recommended.⁷ The energy dissipated during strain hardening $g_{f,A}$, is an energy per unit volume (kJ/m^3) of composite assuming an evenly distributed (multiple) cracking behavior. In comparison, the fracture energy G_f represents the energy per unit ligament area to completely separate the material through a single crack and is given in kJ/m^2 . To calculate $g_{f,A}$, the unloading modulus at maximum stress E_{pc} is needed (refer to the example in Fig. 6(a)). The total energy absorption capacity g of a strain-hardening material prior to softening is the sum of dissipated energy $g_{f,A}$, and elastically stored recoverable energy g_{el} (Eq. (1) and (2)). These energy components per unit volume allow for an objective comparison of the strain-hardening performance of different composites and are mathematically defined as follows

$$g = \int_0^{\varepsilon_{pc}} \sigma(\varepsilon) d\varepsilon = g_{f,A} + g_{el} \quad (1)$$

$$g_{el} = \frac{1}{2} \frac{\sigma_{pc}^2}{E_{pc}} \quad (2)$$

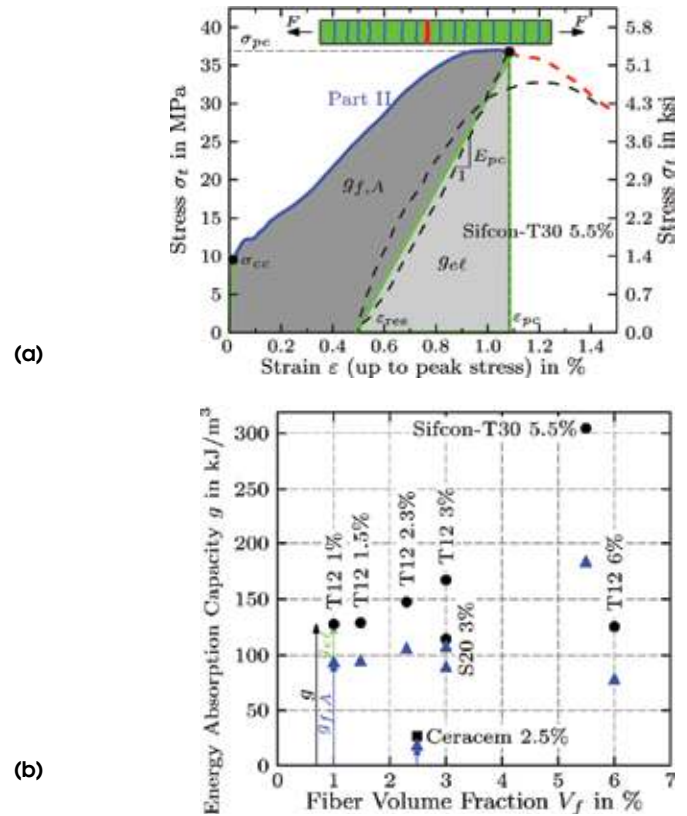


Fig. 6: Energy absorption capacity per unit volume associated with strain hardening behavior: (a) geometric equivalent of $g_{f,A}$ and g_{el} in an example of Sifcon-T30 5.5%; and (b) comparison of g , $g_{f,A}$, and g_{el} of series investigated in this research

Figure 6(a) illustrates the geometric equivalent of $g_{f,A}$ and g_{el} of a typical composite specimen, Sifcon-T30 5.5%. Numerical values of the energy per unit volume for all test series investigated in this study are plotted in Fig. 6(b) as functions of fiber volume fraction. The estimated energy for Ceracem[®] 2.5% is also shown for comparison. In terms of fiber volume effectiveness, UHP-FRC T12 1% exhibits the highest energy absorption capacity per unit volume of composite and per 1% fiber content, namely $g_f = 128 \text{ kJ/m}^3$ and $g_{f,A} \approx 92 \text{ kJ/m}^3$. However, in terms of absolute values, UHP-FRC Sifcon-T30 5.5% leads to the highest values of $g_f = 304 \text{ kJ/m}^3$ and $g_{f,A} \approx 184 \text{ kJ/m}^3$, respectively. Per 1% fiber content, the energy values of the UHP-FRC composites developed in this study are five to 10 times those achieved by Ceracem 2.5%. The energy absorption capacity during softening is not discussed in this article, but its method of computation is described in Wille and Naaman.⁷

Record-Breaking Results

Our research has led to two main developments:

- UHPC mixtures with 28-day compressive strengths in excess of 200 MPa (30 ksi). Significantly, these mixtures

required no heat or pressure curing, incorporated materials available on the U.S. market, and were mixed in a conventional concrete mixer; and

- A UHP-FRC mixture with a tensile strength of over 37 MPa (5.4 ksi). This mixture developed strains as high as 1.1% at maximum stress, and the energy absorption prior to softening was 304 kJ/m³. Before tensile fracture, specimens exhibited multiple cracks, with crack spacing and widths respectively as small as 1 mm (0.04 in.) and 4 microns (1.57×10^{-7} in.).

We believe some of the newly developed mixtures shown in Table 2 and Fig. 5 delivered record-breaking results for cement composites. Mixture T12 1%, for example, with only a 1% volume fraction of steel fibers, developed a tensile strength of 15.9 MPa (2.3 ksi) and an energy absorption capacity of 128 kJ/m³. These values far exceed those reported by other researchers.

Acknowledgments

This work was supported by a fellowship within the Postdoctoral Program of the German Academic Exchange Service (DAAD). The senior authors would also like to acknowledge the support of the

University of Michigan and the National Science Foundation under grant No. CMMI 0754505. We also acknowledge the following companies for providing free material: BASF Construction Chemicals, Bekaert, Chryso Inc., Holcim (US) Inc., Elkem Materials, Grace Construction Products, Lehigh Cement Company, and Sika Corporation. The opinions expressed in this paper are those of the authors and do not necessarily reflect the views of the sponsors.

References

1. Graybeal, B., and Tanesi, J., "Durability of an Ultra-High-Performance Concrete," *Journal of Materials in Civil Engineering*, V. 19, No. 10, 2007, pp. 848-854.
2. Behloul, M.; Bernier, G.; and Cheyrezy, M., "Tensile Behavior of Reactive Powder Concrete (RPC)," *Proceedings of the 4th International Symposium on Utilization of HSC/HPC*, BHP'96, Paris, France, Presses de l'ENPC, V. 3, 1996, pp. 1375-1381.
3. Schmidt, M.; Fehling, E.; Bormeman, R.; and Middenhof, B., "Ultra-Hochleistungs-beton: Herstellung, Eigenschaften und Anwendungsmöglichkeiten (Ultra-High-Performance Concrete: Production, Properties, and Applications)," *Beton- und Stahlbetonbau*, V. 96, 2001, No. 7, pp. 458-467. (in German)

Earn CEUs from the comfort and privacy of your home, office, or anywhere!

ACI offers an easy-to-use online CEU program for anyone that needs to earn Continuing Education credits.

ACI members can take up to eight courses **FREE of charge** per membership year. Nonmembers and members that have used all of their free courses can purchase courses for \$25. Each course includes a 10-question exam.

Participants must register and login to the ACI Web site. Once registered, users can download and study resource materials that the exams are keyed to. After the exam is passed, ACI issues a certificate of completion for presentation to local licensing agencies.

Check it out now! For details go to: www.concrete.org/education/edu_online_CEU.htm

The following are some of the courses that have recently been added to the program:

- **The Contractor's Guide to Quality Concrete Construction, Chapter 8, Joints and Reinforcement for Slabs-on-Ground;**
- **The Contractor's Guide to Quality Concrete Construction, Chapter 10, Concrete Placement and Finishing;** and
- **SP-4 Formwork for Concrete, Chapter 10, Using the Forms.**

In addition, the program includes courses on the following topics:

- **Cracking;**
- **Aggregates;**
- **Admixtures;**
- **Test Reports;**
- **Slabs;**
- **Reinforcement;**
- **Repair;**
- **Shotcrete; and**
- **Foundations;**
- **Cementitious materials;**
- **Shoring;**
- **Formwork.**



4. Chanvillard, G., and Rigaud, S., "Complete Characterisation of Tensile Properties of DUCTAL® UHP-FRC According to the French Recommendations," *Fourth International Workshop on High Performance Fiber Reinforced Cement Composites (HPRCC4)*, 2003.

5. Benson, S.D.P., and Karihaloo, B.L., "CARDIFRC—Development and Mechanical Properties. Part III: Uniaxial Tensile Response and Other Mechanical Properties," *Magazine of Concrete Research*, V. 57, No. 8, 2005, pp. 433-443.

6. Jungwirth, J., and Muttoni, A., "Structural Behavior of Tension Members in UHPC," *Proceedings of the International Symposium on Ultra-High-Performance Concrete*, Kassel, Germany, 2004, pp. 533-544.

7. Wille, K., and Naaman, A.E., "Fracture Energy of UHPFRC under Direct Tensile Loading," *FraMCoS-7 International Conference*, Jeju, Korea, May 23-28, 2010.

8. Wille, K.; Naaman, A.; and Parra-Montesinos, G., "Ultra-High-Performance Concrete with Compressive Strength Exceeding 150 Mpa (22 ksi): A Simpler Way," *ACI Materials Journal*, V. 108, No. 1, Jan.-Feb. 2011, pp. 46-54.

9. Wille, K.; Kim, D.; and Naaman, A.E., "Strain-Hardening UHP-FRC with Low Fiber Contents," *Materials and Structures*, V. 44, No. 3, 2011, pp. 583.

10. Rossi, P., "Ultra-High-Performance Concretes," *Concrete International*, V. 30, No. 2, Feb. 2008, pp. 31-34.

11. Kamal, A.; Kunieda, M.; Ueda, N.; and Nakamura, H., "Evaluation of Crack Opening Performance of a Repair Material with Strain Hardening Behavior," *Cement and Concrete Composites*, V. 30, 2008, pp. 863-871.

12. Wille, K., and Naaman, A.E., "Bond Stress Slip Hardening Behavior of Steel Fibers Embedded in Ultra-High-Performance Concrete," 18th European Conference on Fracture, Dresden, Germany, Aug. 30-Sept. 3, 2010.

13. Chan, Y.-W., and Chu, S.-H., "Effect of Silica Fume on Steel Fiber Bond Characteristics in Reactive Powder Concrete," *Cement and Concrete Research*, V. 34, No. 7, 2004, pp. 1167-1172.

14. Lee, Y.; Kang, S.T.; and Kim, J.K., "Pullout Behavior of Inclined Steel Fiber in an Ultra-High Strength Cementitious Matrix," *Construction and Building Materials*, V. 24, No. 10, Oct. 2010, pp. 2030-2041.

15. Markovic, I., "High-Performance Hybrid-Fibre Concrete—Development and Utilisation," Delft University of Technology, Delft, the Netherlands, PhD thesis, 2006, 232 pp.

16. Naaman, A.E., and Wille, K., "Some Correlation between High Packing Density, Ultra-High Performance, Flow Ability, and Fiber Reinforcement of a Concrete Matrix," *BAC2010—2nd Iberian Congress on Self Compacting Concrete*, University of Minho-Guimaraes, Portugal, July 1-2, 2010.

17. Lankard, D., "Slurry Infiltrated Fiber Concrete (SIFCON): Properties and Applications," *Very High Strength Cement-Based Materials*, J.F. Young, ed., *Materials Research Society Symposium Proceedings*, V. 42, Pittsburgh, PA, 1985, pp. 277-286.

18. Naaman, A.E., "SIFCON: Tailored Properties for Structural Performance," *High Performance Fiber Reinforced Cement Composites*,

H.W. Reinhardt and A.E. Naaman, eds., *RILEM Proceedings 15*, E&FN Spon, London, UK, 1992, pp. 18-38.

19. Boulay, C.; Rossi, P.; and Tailhan, J.-L., "Uniaxial Tensile Test on a New Cement Composite Having a Hardening Behaviour," *Sixth RILEM Symposium in Fibre-Reinforced Concretes (FRC)*, BEFIB 2004, Varenna, Italy, 2004.

20. Orange, G.; Dugat, J.; and Acker, P., "DUCTAL: New Ultra-High-Performance Concretes. Damage, Resistance and Micromechanical Analysis," *BEFIB 2000, Fifth RILEM Symposium on Fiber-Reinforced Concretes (FRC)*, P. Rossi and G. Chanvillard, eds., Lyon, France, 2000, pp. 781-790.

21. Rossi, P.; Acker, P.; and Malier, Y., "Effect of Steel Fibres at Two Stages: The Material and the Structure," *Materials and Structures*, V. 20, No. 6, 1987, pp. 436-439.

Received and reviewed under Institute publication policies.



ACI member **Kay Wille** is an Assistant Professor in the Department of Civil and Environmental Engineering at the University of Connecticut, Storrs. Formerly a Postdoctoral Fellow at the University of Michigan, Ann Arbor, he is a member of ACI Committee 544, Fiber-Reinforced Concrete. His research interests include design, analysis, and modeling of ultra-high-performance concrete and fiber-reinforced cement composites under static and high strain rate tensile loading.



Antoine E. Naaman, F.A.C.I., is a Professor Emeritus of Civil and Environmental Engineering at the University of Michigan, Ann Arbor. He is a member of ACI Committees 544, Fiber-Reinforced Concrete; 549, Thin Reinforced Cementitious Products and Ferrocement; and consulting member of Joint ACI-ASCE

Committee 423, Prestressed Concrete. His research interests include high-performance fiber-reinforced cement composites, ferrocement, and prestressed concrete.



Sherif El-Tawil is a Professor of Civil and Environmental Engineering at the University of Michigan, Ann Arbor. His research interests include high strain rate material response, ultra-high-performance fiber-reinforced cement composites, and computational simulation of material and structural responses.